Molecular BioSystems

Accepted Manuscript

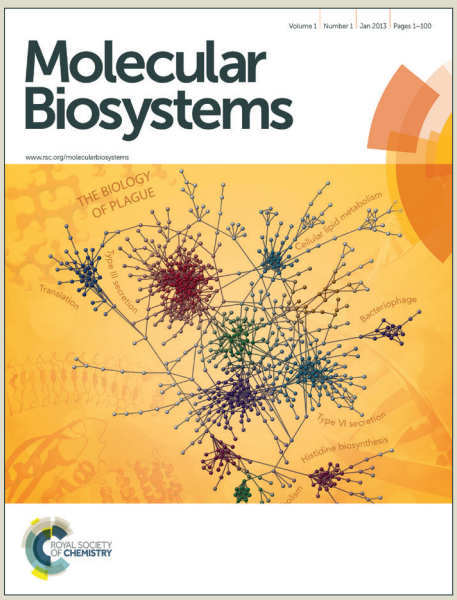

ROYAL SOCIETY OF CHEMISTRY

www.rsc.org/molecularbiosystems

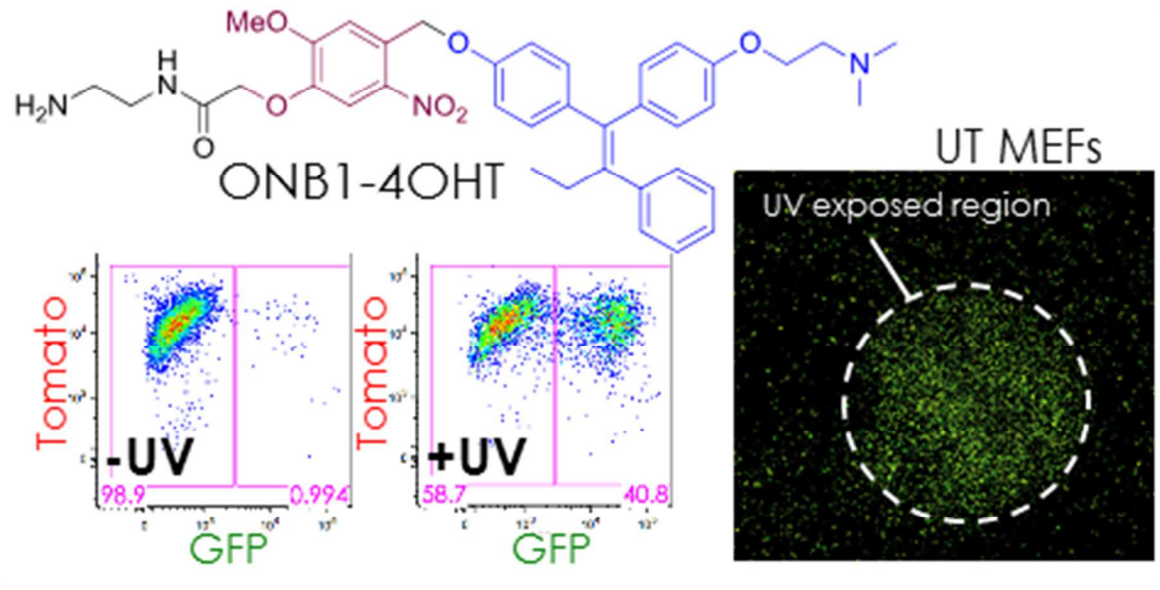

Here, we synthesized and validated a photocaged hydroxytamoxifen molecule to achieve spatiotemporal control of gene expression with light.

Molecular Biosystems

RSCPublishing

ARTICLE

4-Hydroxytamoxifen probes for light-dependent spatiotemporal control of Cre-ER mediated reporter gene expression

Cite this: DOI: 10.1039/x0xx00000x

Received 00th January 2012,
Accepted 00th January 2012

DOI: 10.1039/x0xx00000x

www.rsc.org/

Tannaz Faal,[1,2,†] Pamela T. Wong,[3,†] Shengzhuang Tang,[3] Alexa Coulter,[3] Yumay Chen,[1,4] Christina H. Tu,[1] James R. Baker, Jr.,[3] Seok Ki Choi,[3,*] and Matthew A. Inlay[1,2,*]

The tamoxifen inducible Cre-ER/loxP system provides tissue specific temporal control of gene recombination events, and can be used to induce expression of reporter genes (e.g. GFP, LacZ) for lineage tracing studies. Cre enzyme fused with estrogen receptor (Cre-ER) is released upon tamoxifen binding, resulting in permanent activation of reporter genes within cells and their progeny. Tamoxifen and its active metabolite, hydroxytamoxifen (4OHT) diffuses rapidly *in vivo*, making it difficult to restrict labeling to specific locations. In this study, we developed a photocaged 4OHT molecule by covalently attaching 4OHT to an ortho-nitrobenzyl (ONB_1) group, rendering 4OHT inactive. Exposure to UV radiation cleaves the bond between ONB_1 and 4OHT, freeing the 4OHT to bind Cre-ER to result in downstream genetic recombination and reporter activation. We show that caged ONB_1-4OHT crosses the cell membrane and uncages after short UV exposure, resulting in Cre-driven genetic recombination that can be localized to specific regions or tissues. ONB_1-4OHT can provide spatial control of reporter activation and be adapted with any existing Cre-ER/loxP based system.

Introduction

The ability to selectively mark cells and track their progeny, called lineage tracing, has been used to answer key questions in lineage commitment and fate determination. Activation of reporter genes can be restricted to specific target cells by choice of tissue-specific promoters that control Cre expression. Discovery of the P1 bacteriophage tyrosine recombinase enzyme (Cre recombinase) led to the development of promoter-specific Cre models allowing for cell type-specific gene expression. Cre recognizes and binds to 34bp DNA sequences called loxP sites, and drives DNA recombination for the permanent activation or deletion of a gene flanked by two loxP sites[1]. Fusion of Cre to the estrogen receptor (ER) sequesters Cre-ER in the cytoplasm until bound by the estrogen analog 4-hydroxytamoxifen (4OHT).[2-5] While 4OHT can be topically applied to or injected into a specific region, 4OHT rapidly penetrates into the blood stream and can activate Cre recombination far beyond the injection site. As a result, spatiotemporal control of reporter activation has remained elusive as a lineage-tracing tool.

Photocaging technology may offer a means to localize reporter induction to specific regions. Photocaging is a process of rendering a molecule inert by covalent attachment of a photocaging group.[6, 7] Reporter expression can be localized to a specific region upon direct exposure to a specific wavelength of light, which releases and activates the photocaged molecule. Photocaging has been used in a variety of applications from studies of transcription,[8] protein-protein interactions,[9, 10] cell migration and proliferation,[11] protein phosphorylation,[12] and targeted drug delivery,[13-16] as well as gene expression using Cre-ER.[17-21]

We previously published a study validating this concept using a photocaged tamoxifen (TAM).[22] In that study, an o-nitrobenzyl (ONB)-alkylated N-quaternary salt[15, 23, 24] of tamoxifen (ONB-TAM) was synthesized and found to be water soluble, and its activity was neutralized until exposed to long wave ultraviolet light (UVA, 365 nm). We also generated a reporter, called UT MEFs, from mouse embryonic fibroblasts and used it to validate the activity of ONB-TAM. UT MEFs combined a constitutively expressed Cre-ER^{T2} (driven by the Ubiquitin C promoter),[25] and an mTmG reporter construct that switches from Tomato to GFP fluorescence when Cre is activated,[26] and could reliably detect photoreleased TAM by induction of GFP expression. However, ONB-TAM had difficulties that limited its use. Because TAM does not bind Cre-ER directly, but rather must first be converted to 4OHT by cell-type specific enzymes, its use was restricted to cells like

MEFs which are capable of converting TAM to 4OHT. Furthermore, *in vitro* this conversion was inefficient and ONB-TAM required near toxic concentrations in order to achieve robust reporter activation.

Results and Discussion

To develop a more efficient and sensitive light-activated reporter system, we focused our attention on photocaging 4OHT. We designed two ONB-based photocaged 4OHT molecules—ONB_1-4OHT 1 and ONB_2-4OHT 2—by covalent linkage of 4OHT (Z and E isomers) at its phenolic moiety to an ONB cage (Fig. 1). However, these two photoprobes are distinguished by nature of their linkage in which ONB_1-4OHT was prepared via direct *O*-alkylation while ONB_2-4OHT was prepared via formation of an extended carbamate spacer (Scheme 1, 2). Each of the products was fully characterized by mass spectrometry (ESI, HRMS), NMR (^{1}H) spectroscopy, and UV–vis spectrophotometry (see details in Supplementary Information Figures 1-4). The purity of each ONB-4OHT was determined by analytical HPLC as >98% without detectable free 4OHT (Fig. 1, Supplementary Fig. 1). It is noteworthy that use of an ONB linker S1 (Scheme 1) for this design allowed us to photocage 4OHT as well as greatly improve the aqueous solubility of the resulting ONB_1-4OHT or ONB_2-4OHT (≥20 mg/mL) compared to the practically insoluble 4OHT (≈0.0002 mg/mL water[27]). We believe that such favorable solubility is attributable to the positively charged amine-terminated side chain tethered to the ONB group.

We investigated whether exposure of ONB_1-4OHT and ONB_2-4OHT to UV light would trigger release of 4OHT (Fig. 1b) or its carbamate derivative S8 (Supplementary Fig. 1). HPLC analysis of photolysed solutions (Fig. 1b,c) indicates that drug release occurs in a time-dependent manner and results in ~90% released after 5 min (ONB_1-4OHT) and ~15 min (ONB_2-4OHT). Release was also confirmed by mass spectrometric analysis of the same UV-treated solutions, which showed an increase in peaks corresponding to free 4OHT ($[M+H]^+$ = 388.2; Supplementary Fig. 2) and S8 ($[M+H]^+$ = 502.3; Supplementary Fig. 3). These results suggest that ONB_1-4OHT has advantages over ONB_2-4OHT for drug release based on its greater release rate. In addition, ONB_1-4OHT releases free 4OHT directly while ONB_2-4OHT releases first S8, a 4OHT derivative which is expected to undergo intramolecular self immolation[28] through its methyl(2-(methylamino)ethyl)carbamate to release free 4OHT in the cell. As proof of concept, we next used confocal fluorescence imaging to confirm photoactivation of ONB-4OHT compounds by UVA exposure of UT MEF reporter cells (Fig. 1d). In the UT MEF system, cells constitutively express Tomato until uncaged 4OHT drives Cre-ER mediated recombination to delete the Tomato gene and activate GFP expression. UT MEFs were treated with 5 μM of 4OHT, ONB_1-4OHT, or ONB_2-4OHT, exposed to UVA for 5 min, and imaged after 24 h of incubation. Cells alone and cells treated with ONB_1-4OHT and ONB_2-4OHT without UV treatment showed no GFP fluorescence. However, cells treated with free 4OHT had significant GFP expression with or without UV exposure. Upon UV exposure, cells treated with ONB_1-4OHT or ONB_2-4OHT showed a large increase in GFP fluorescence, whereas UT MEFs alone showed minimal GFP expression. These results support UVA-induced 4OHT release from the ONB constructs, and the ability of the released 4OHT moiety to activate recombination through Cre-ER.

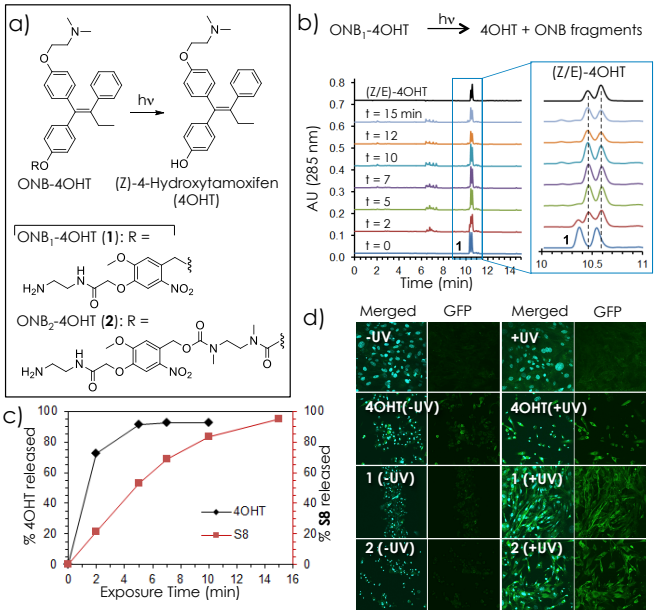

Figure 1. (a) Structures of two ortho-nitrobenzyl (ONB)-caged 4-hydroxytamoxifen (4OHT) molecules, and a photochemical mechanism for release of 4OHT; (b) HPLC traces indicative of UVA-controlled release of 4OHT from ONB1-4OHT (10% aq MeOH) as a function of exposure time; (c) plots of photochemical release kinetics of 4OHT (%AUC from HPLC traces in B) or S8 (see Figure S1, Supporting Information), each from ONB1-4OHT **1** or ONB2-4OHT **2**, respectively; (d) Photo-controlled release of 4OHT or S8 for Cre-ER mediated GFP expression in UT MEF cells. Cells were treated with media (top), 4OHT, ONB1-4OHT **1** or ONB2-4OHT **2** without (left panels) or with (right panels) UV exposure. "Merged" columns show DAPI and GFP fluorescence, "GFP" columns show GFP alone.

While we previously used the UT MEF reporter system to validate the photorelease of photocaged TAM,[22] it required near toxic concentrations (≥8 μM). Consequently, our initial test of ONB-4OHT compounds used similarly high concentrations (5 μM), and we often observed reduced cell viability after treatment (Fig. 1d). Therefore, we sought to re-optimize conditions for use with photocaged 4OHT. We first tested unmodified 4OHT for recombination efficiency (as detected by percentage of GFP^+ cells 24 h after initiation of treatment by flow cytometry) and MEF viability (by the absolute number of cells in each condition after 24 h) varying 4OHT concentration (Supplementary Fig. 5a,b), 4OHT treatment time (Supplementary Fig. 5c), serum concentration (Supplementary Fig. 6), and UV exposure time (Supplementary Fig. 7). We determined that 4OHT induces robust recombination at concentrations as low as 15 nM, and after treatment times as

short as 15 min. Furthermore, neither recombination efficiency nor MEF viability are affected by serum concentration or UV exposure. Thus, the UT MEF reporter system provides an efficient means to study the photorelease of photocaged 4OHT. We next optimized conditions with photocaged 4OHT (Fig. 2).

We began with the faster release ONB_1-4OHT, and exposed varying concentrations of ONB_1-4OHT to UVA (365 nm) for 5 min before adding them to UT MEFs. Following 24 h treatments with UV-exposed ONB_1-4OHT, UT MEFs displayed robust GFP activation at all tested concentrations (Fig. 2b,c), similar to the percentage of GFP-expressing cells treated with 1 μM 4OHT. In the absence of UV exposure, we observed significant background recombination at high concentrations of ONB_1-4OHT (500 nM and 1 μM), indicating that either a low percentage of ONB_1-4OHT is uncaged, spontaneously uncages, or has a low efficiency of binding to Cre-ER. However, little to no background recombination was observed in ONB_1-4OHT concentrations at or below 240 nM. We also observed no significant decrease in UT MEF viability, indicating that neither ONB_1-4OHT nor its UV-exposed byproducts are toxic (Fig. 2c). We also examined a range of UV exposure times from 30 s to 20 min and observed robust GFP reporter activation at all times, with no effect on cell viability (Fig. 2d). We tested multiple concentrations and UV exposure times and determined that 240 nM and 1 min UV exposure was optimal for uncaging ONB_1-4OHT with minimal background recombination (Fig. 2e).

We next compared ONB_1-4OHT to ONB_2-4OHT with 1 min UV exposure and a wide range of concentrations (Supplementary Fig. 8). The efficiency of GFP reporter activation was substantially less with ONB_2-4OHT compared to ONB_1-4OHT, and at 1 μM, background recombination was evident with ONB_2-4OHT, indicating this molecule does not uncage efficiently upon UV exposure. We thus pursued only ONB_1-4OHT for the remainder of our experiments.

ONB_1-4OHT can be efficiently uncaged by exposure to UV light, and once uncaged, can rapidly penetrate UT MEFs and activate recombination. Since this photo-inducible system will be used for spatial activation *in vivo*, it is necessary to deliver ONB_1-4OHT into cells in its caged inactive form, *then* uncage it directly inside target cells. Thus, we next determined whether incubation of UT MEFs with the caged form of ONB_1-4OHT followed by direct exposure of UT MEFs to UV light could efficiently allow intracellular uncaging and subsequent reporter activation (Fig. 3). We incubated various concentrations of ONB_1-4OHT with UT MEFs for 1 h at 37 °C, washed cells to remove unbound ONB_1-4OHT, then directly exposed treated cells to 0, 1, or 5 min of UV light (Fig. 3). GFP recombination was observed at all tested concentrations of ONB_1-4OHT that were exposed to UV light (Fig. 3c). Despite directly exposing UT MEFs to UV light, we observed no decrease in viability at any ONB_1-4OHT concentration or UV exposure length. We also examined shorter UV exposure times and observed induction in as little as 15 s of exposure, though the efficiency was reduced compared to longer UV times (Supplementary Fig. 9). Lastly, we tested whether serum concentrations affected ONB_1-4OHT activity, as it did for ONB-TAM,[22] and observed no dramatic difference in recombination efficiency (Supplementary Fig. 10). Our data clearly indicate that the caged form of ONB_1-4OHT can enter UT MEFs with high efficiency, and once inside can be effectively uncaged and induce genetic recombination upon exposure to UV light.

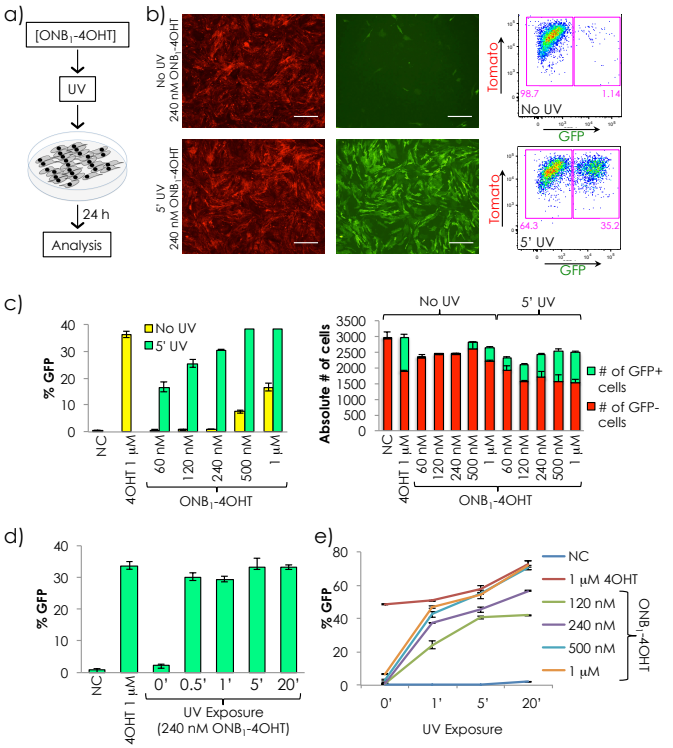

Figure 2. UV uncaging of ONB_1-4OHT and activation of GFP expression in UT MEFs. (a) ONB_1-4OHT was unexposed or exposed to 5 min of UV light (UV-A, 365 nm), then added to and incubated overnight with UT MEFs. (b) Fluorescent images and FACS analysis of UT MEFs treated overnight with either caged ("No UV", top row) or uncaged ("5' UV", bottom row) forms of ONB_1-4OHT (240 nM). All UT MEFs express Tomato at this timepoint, but only those that undergo Cre-mediated recombination express GFP. White bar is 500 microns. (c) Percentage of GFP expressing cells (left graph) and absolute cell number of GFP^+ (green) and GFP^- (red) cells (right graph) at various concentrations of ONB_1-4OHT, unexposed or exposed to UV light. Error bars are standard deviation (N = 3). Untreated UT MEFs were analyzed as a negative control (NC), and 1 μM 4OHT treated UT MEFs were analyzed as a positive control. (d) ONB_1-4OHT (240 nM) was unexposed or exposed to UV for a range of times, then incubated overnight with UT MEFs. Percentage of GFP expressing cells is shown with error bars (SD, N = 3). (e) Comparison of ONB_1-4OHT concentrations and UV exposure times. Percentage of GFP expressing cells is shown with error bars (SD, N = 3).

To validate ONB_1-4OHT in a separate *in vitro* reporter system, we generated a second 4OHT-inducible reporter MEF line by crossing reporter mouse strains that collectively contain 3 genetic modifications: 1) A Cre-ER transgene under control of a constitutively expressed chicken β-actin promoter (Actin-CreER),[29] 2) a Cre-activated LacZ reporter inserted into the Rosa26 locus (R26R),[30] and 3) a Rainbow reporter, also

inserted into the Rosa26 locus, which initially expresses GFP but will recombine to delete GFP and stochastically induce either Cerulean (CFP), mOrange (OFP), or TdTomato (RFP) fluorescent protein expression upon Cre-mediated recombination[31] (Supplementary Fig. 11). Using similar experimental strategies described for UT MEFs, we tested Actin-CreER x Rainbow x LacZ MEFs (hereafter called ACRL MEFs) for 4OHT and ONB_1-mediated reporter induction (Supplementary Fig. 12, 13). To characterize 4OHT-mediated reporter induction, we treated ACRL MEFs with 1 μM 4OHT for 1 hr then left in culture for up to 9 days. Robust expression of LacZ was observed after 24 hrs following 4OHT treatment (Supplementary Fig. 12a). A time course experiment was performed to determine optimal treatment time for Rainbow reporter induction. After treatment with 1 μM 4OHT, ACRL MEFs were cultured between 24 hours and 9 days. We found that GFP expression began to diminish and CFP, OFP, and RFP recombination began to increase after 3 days, with the highest percent recombination observed at 7 days. (Supplementary Fig. 12b, c). We next determined ONB_1-mediated reporter induction by incubating ACRL MEFs with 120nM or 240nM ONB_1-4OHT for 1 h at 37°C then washed to remove unbound ONB_1-4OHT (Supplementary Fig. 13). Cells treated with ONB_1 were then directly exposed to 1 min UV light. We observed robust induction of LacZ expression in ONB_1-4OHT UV treated cells after 24 hours (Supplementary Fig. 13a) and Rainbow induction after 7 days (Supplementary Fig. 13b, c). Thus, ONB_1-4OHT can confer light-activated reporter gene induction in two distinct *in vitro* reporter systems and 3 distinct reporter genes.

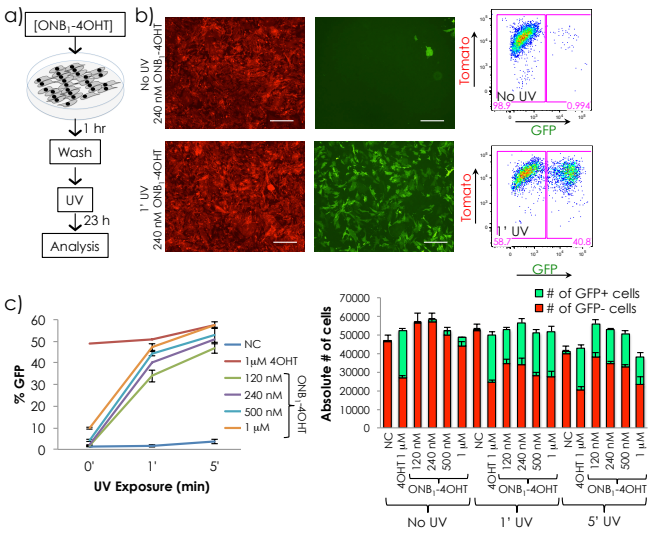

Figure 3. Uncaging ONB_1-4OHT after entry into UT MEFs. (a) UT MEFs were treated with caged ONB_1-4OHT for 1 h to allow entry into the cells, then washed and exposed to UV light to uncage only intracellular ONB_1-4OHT. (b) Representative fluorescent images and FACS analysis are shown for the activation of GFP and the presence of Tomato for caged ("No UV", top row) and intracellularly uncaged ("1' UV", bottom row) forms of ONB_1-4OHT. White bar is 500 microns. (c) Graphs for GFP expressing cells and absolute cell number at different ONB_1-4OHT concentrations and UV exposure times. Error bars are SD (N = 3).

Our goal for ONB_1-4OHT is to use it to activate reporter expression in a specific region by exposing only that region to UV light. To demonstrate this spatial activation, we plated UT MEFs on glass bottom tissue culture dishes, treated the confluent cells for 1 h with 240 nM ONB_1-4OHT, washed the plate to remove unbound ONB_1-4OHT, and directly exposed only a specific region of the UT MEFs to UV light for 1 min using an opaque non-reflective cylinder placed directly above the dish (Fig. 4a). We observed significantly high activation of GFP expression only in the cells that resided within the region

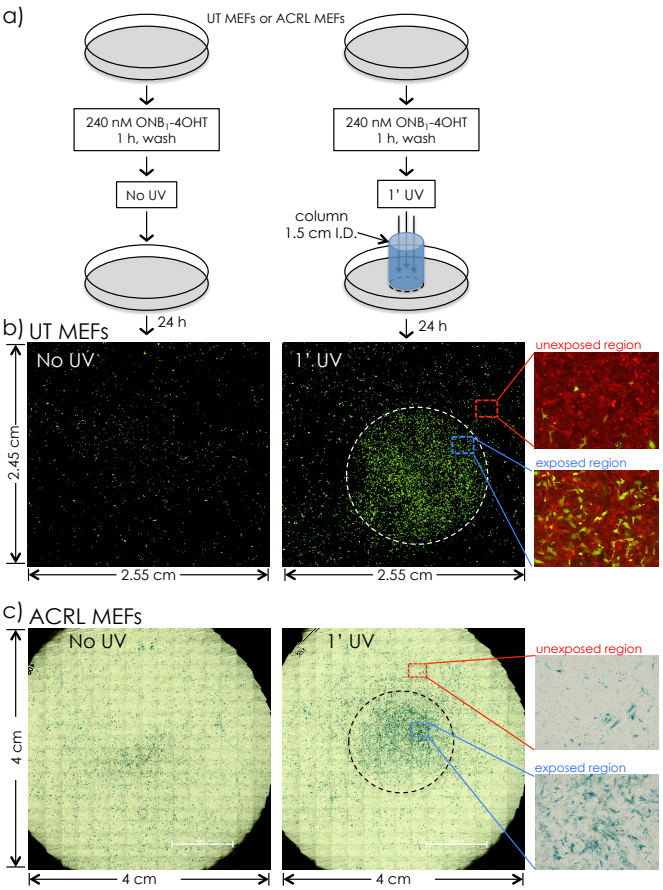

Figure 4. Spatial activation of GFP expression in UT MEFs and LacZ expression in ACRL MEFs. (a) UT MEFs were plated on glass bottom dishes and treated with 240 nM ONB_1-4OHT for 1 h, then washed. A circular column (blue column, 1.5 cm inner diameter) was placed above the dish directly above a region of cells, which was then exposed to UV light for 1 min. Cellular GFP fluorescence was imaged after 24 h. (b) 2.55 cm × 2.45 cm regions of dishes treated with ONB_1-4OHT and either unexposed (left) or exposed (middle) to UV light. Images are composites of 120 separate photographs. (c) ACRL MEFs were plated on 6cm dishes and treated as described above. Cellular LacZ was imaged after 24 h. 4 cm × 4 cm regions of dishes treated with ONB_1-4OHT were either unexposed (left) or exposed (middle) to UV light. Images are composites of 300 separate photographs. The black broken circle indicates the region exposed to UV light. The white broken circle indicates the region exposed to UV light. Zoomed-in images of an unexposed region (red box, top right) and exposed region (blue box, left) revealing both GFP (green cells) or LacZ (blue cells) induction, as well as non-rearranged cells (red cells or unstained) indicating that both regions were equally confluent.

directly exposed to UV light (Fig. 4b). While a low level of background GFP induction was observed in cells outside of the exposed region, it was similar to a control plate that was treated with 240 nM ONB_1-4OHT without UV exposure (Fig. 4b). Thus, ONB_1-4OHT can induce reporter expression within specific regions of a dish by restricted exposure to UV light. We repeated this experiment using the ACRL MEFs plated on a 6 cm dish and imaged for LacZ expression (Fig. 4c). We observed robust genetic recombination only within the region exposed to UV light. We conclude that using ONB_1-4OHT and UT MEF and ACRL MEF reporter cells, we have achieved spatiotemporal control of reporter gene activation *in vitro*.

Conclusions

We demonstrated light-activated gene expression by photocaging 4OHT and validated its activity on UT and ACRL MEFs. We believe that this study significantly advances the field of photo-inducible Cre-ER reporter labeling in several aspects. First, unlike earlier reports suggesting the photodegradability of 4OHT,[20] the current result shows that 4OHT itself is functionally photostable and useful for UV-based photocaging. Second, we find that photocaged 4OHT is over 100-fold more active than photocaged TAM, can efficiently enter UT MEFs in its caged form and be activated intracellularly, and as a result can be used to induce reporter expression in a specific region by focused light exposure. Third, in addition to our previously published UT MEF reporter line, we introduce ACRL MEFs as another tool for validating new lineage-tracing technologies. Fourth, our current results demonstrate that 4OHT-based photocaging technology is capable of conferring spatiotemporal control of reporter activation *in vitro*.

Many studies describing light-inducible genetic recombination require the modification of existing transgenes.[32] Our photocaged system does not require further modifications and can potentially be applied to any existing Cre-ER or Cre-ER^{T2} reporter system. Our future efforts will focus on validating the efficiency of this photocaged 4OHT molecule for spatiotemporal reporter activation *in vivo*.

Materials and Methods

Chemistry, General. All solvents and reagents were purchased from Sigma-Aldrich and other commercial suppliers, and used without further treatment. Thin layer chromatography was performed on Merck® TLC plates (250 μm thick), and migration spots were detected by UV lamp illumination or by staining with phosphomolybdic acid reagent (20% w/v in ethanol) or ninhydrin solution (5% w/v in 3% acetic acid/ethanol). Flash column chromatography was performed using silica gel (200-400 mesh) by eluting with solvent eluents as specified in each of the reactions.

Each reaction was performed in the dark (with individual reaction container wrapped with aluminum foil) unless noted otherwise. Spectral characterization of reaction products was carried out by a combination of ^{1}H NMR spectroscopy, mass spectrometry and UV–vis spectrophotometry. For NMR (^{1}H, ^{13}C) measurement, each sample solution was prepared by dissolving in the deuterated solvent ($CDCl_3$, CD_3OD, DMSO-d_6, D_2O), and its spectra were acquired with a Varian nuclear magnetic resonance spectrometer at 400 MHz or 500 MHz for ^{1}H NMR spectra, and at 100 MHz for ^{13}C NMR spectra under standard observation conditions. For mass spectrometric characterization of compounds, electrospray ionization mass spectrometry (ESI-MS) was performed with a Micromass AutoSpec Ultima spectrometer. UV–vis absorption spectra were acquired with a Perkin Elmer Lamda 20 spectrophotometer.

HPLC analysis was performed on a Waters Ultra Performance Liquid Chromatography System equipped with a Waters photodiode array detector, a column manager that facilitates 4 column housing, and a sample manager. Each sample solution was run on a C4 BEH column (150 × 2.1 mm, 300 Å) connected to a Waters Vanguard column. Elution was performed in a linear gradient manner beginning with 98:2 (v/v) water/acetonitrile (with trifluoroacetic acid at 0.14 wt % in each eluent) at a flow rate of 1 mL/min.

I. Synthesis of ONB_1-4OHT 1 (Scheme 1)

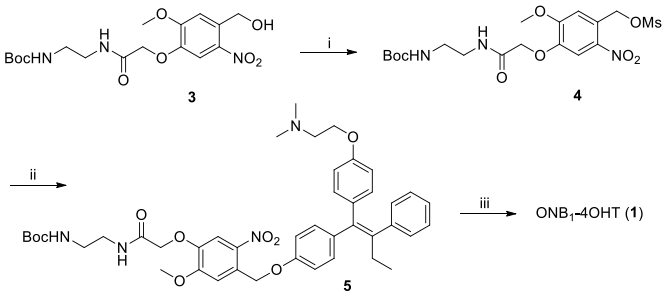

reagents and conditions: i) Methanesulfonyl chloride (MsCl), Et_3N, CH_2Cl_2, 0°C to rt; ii) 4OHT, K_2CO_3, Cs_2CO_3, DMF, rt to 60°C; iii) CF_3CO_2H, CH_2Cl_2, rt, 30 min

4-Hydroxytamoxifen (**4OHT**): A batch of 4OHT (100 mg scale) was prepared according to a literature procedure[33] based on the McMurry reaction. 4OHT was synthesized as a mixture of Z and E isomers (1:1), and identified by ^{1}H NMR spectroscopy and ESI mass spectrometry. HPLC analysis of the product indicated the presence of two isomers as two resolved peaks with their retention times (t_R) identical to those acquired from commercial 4OHT Z and E isomers (1:1; Sigma-Aldrich). HPLC: t_R = 10.5, 10.6 min; purity >98%. MS (ESI) *m/z* (relative intensity, %) = 388.3 (100) $[M+H]^+$. ^{1}H NMR (500 MHz, CD_3OD): δ 7.16–7.06 (m, 6H), 7.02–6.70 (dd, J_1 = 2 Hz, J_2 = 6.5 Hz, 1H), 6.94–6.92 (dd, J_1 = 2.5 Hz, J_2 = 7 Hz, 1H), 6.76–6.74 (dd, J_1 = 2 Hz, J_2 = 6.5 Hz, 2H), 6.64–6.63 (dd, J_1 = 2 Hz, J_2 = 7 Hz, 1H), 6.57–6.56 (dd, J_1 = 2 Hz, J_2 = 6.5 Hz, 1H), 6.40–6.38 (dd, J_1 = 2 Hz, J_2 = 6.5 Hz, 1H), 4.15–4.13 (t, J = 5.5 Hz, 1H), 3.98–3.96 (t, J = 5.5 Hz, 1H), 2.86–2.84 (t, J = 5.5 Hz, 1H), 2.77–2.75 (t, J = 5.5 Hz, 1H), 2.49–2.450 (q, J = 7.5 Hz, 2H), 2.41 (s, 3H), 2.34 (s, 3H), 0.91–0.88 (t, J = 7 Hz, 3H) ppm.

4: To cold solution of *tert*-butyl (2-(2-(4-(hydroxymethyl)-2-methoxy-5-nitrophenoxy)acetamido)ethyl)carbamate[15, 22-24] (**3**; 200 mg, 0.501 mmol) dissolved in dichloromethane (15 mL) was added triethylamine (0.147 mL, 1.05 mmol) and then methanesulfonyl chloride (0.043 mL, 0.551 mmol). The mixture was stirred at 5°C in an ice bath for 10 min and at room temp. The reaction progress was monitored by TLC, and when the starting material was fully consumed to a single new spot (~2 h), the mixture was washed with

1M H_3PO_4, a saturated $NaHCO_3$ solution and water. Drying over Na_2SO_4, and subsequent evaporation of the organic solution afforded **4** as pale yellow solid (213 mg, 89%). This product was used in the next step without further treatment. R_f (5% CH_3OH/EtOAc) = 0.67**.**

5: (*N*-Boc protected ONB_1-4OHT): To a solution of 4OHT (20 mg, 51.7 μmol) dissolved in DMF (2 mL) was added K_2CO_3 (21 mg, 155 μmol), Cs_2CO_3 (50 mg, 155 μmol) and then **4** (49 mg, 103 μmol). The mixture was stirred at room temp for 2 h, and then at 60°C for 12 h. After cooling, the mixture was concentrated *in vacuo*, and the residue was partitioned between dichloromethane (5 mL) and water (5 mL). The organic layer was collected, dried over Na_2SO_4, and evaporated to afford a crude product mixture. It was purified by flash silica column chromatography by eluting with 2–5% MeOH in CH_2Cl_2. The product **5** was obtained as pale yellow solid (25.2 mg, 49%). R_f (10% CH_3OH/CH_2Cl_2) = 0.38. MS (ESI) *m/z* (relative intensity, %) = 769.7 (100) $[M+H]^+$. HRMS (ESI) calcd for C43H53N4O9 $[M+H]^+$ 769.3807, found 769.3815. ^{1}H NMR (500 MHz, $CDCl_3$): δ 7.82 (s, 0.5H, ArH ortho to NO_2), 7.77 (s, 0.5H, ArH ortho to NO_2), 7.45 (s, 0.5H, ArH meta to NO_2), 7.32 (s, 0.5H, ArH meta to NO_2), 7.19–7.09 (m, 7H, ArH), 7.00–6.98 (d, *J* = 9 Hz, 1H, ArH), 6.91–6.89 (d, *J* = 8.5 Hz, 1H, ArH), 6.82–6.80 (d, *J* = 9 Hz, 1H, ArH), 6.76–6.75 (d, *J* = 8.5 Hz, 1H, ArH), 6.66–6.64 (d, *J* = 8.5 Hz, 1H, ArH), 6.56–6.55 (d, *J* = 9 Hz, 1H, ArH), 5.52 (s, 1H, Ar**CH$_2$**O), 5.37 (s, 1H, Ar**CH$_2$**O), 4.89 (br, 1H, **NH**), 4.59 (s, 1H, ArO**CH$_2$**C(=O)), 4.56 (s, 1H, ArO**CH$_2$**C(=O)),4.13–4.11 (t, *J* = 5.5 Hz, 1H, **CH$_2$O**), 3.99 (s, 1.5H, **CH$_3$O**), 3.98–3.96 (t, 1H, *J* = 6 Hz **CH$_2$O**), 3.91 (s, 1.5H, **CH$_3$O**), 3.51–3.46 (m, 2H, CH_2N), 3.33–3.31 (m, 2H, **CH$_2$**N), 2.82–2.80 (t, *J* = 5 Hz, 1H, **CH$_2$**N), 2.73–2.71 (t, *J* = 5.5 Hz, 1H, **CH$_2$**N), 2.49–2.45 (m, 2H, **CH$_2$**(CH_3)), 2.40 (s, 3H, **CH$_3$**N), 2.34 (s, 3H, **CH$_3$**N), 1.42 (s, 4.5H, NH**Boc**), 1.41 (s, 4.5H, NH**Boc**), 0.94–0.91 (t, *J* = 7.5 Hz, 3H, $CH_3(CH_2)$) ppm. ^{13}C NMR (100 MHz, $CDCl_3$): δ 187.99, 184.63, 162.94, 132.12, 131.85, 130.80, 130.53, 129.64, 127.85, 115.14, 114.61, 114.06, 113.80, 113.32, 67.35, 45.65, 28.28, 19.54 ppm.

1 (ONB_1-4OHT): To *N*-Boc protected ONB_1-4OHT **5** (10 mg) was added slowly a mixture of trifluoroacetic acid (TFA) and dichloromethane (1:1; 6 mL). The solution was stirred at room temp for 30 min, and evaporated to dryness. The pale yellow oily residue was dissolved in 20% aq acetonitrile solution (2 mL), and freeze-dried, yielding pale beige fluffy solid. HPLC: t_R = 10.37, 10.54 min; purity >98% (quantitative deprotection). MS (ESI) *m/z* (relative intensity, %) = 669.4 (11) $[M+H]^+$, 326.7 (100). ^{1}H NMR (500 MHz, CD_3OD): δ 7.88 (s, 0.5H, ArH ortho to NO_2), 7.84 (s, 0.5H, ArH ortho to NO_2), 7.48 (s, 0.5H, ArH meta to NO_2), 7.32 (s, 0.5H, ArH meta to NO_2), 7.20–7.02 (m, 9H, ArH), 6.83–6.78 (m, 2H, ArH), 6.67–6.64 (m, 2H, ArH), 5.49 (s, 1H, Ar**CH$_2$**O), 5.34 (s, 1H, Ar**CH$_2$**O), 4.68 (s, 1H, ArO**CH$_2$**C(=O)), 4.65 (s, 1H, ArO**CH$_2$**C(=O)),4.37–4.35 (t, *J* = 5 Hz, 1H, **CH$_2$**O), 4.21–4.19 (t, 1H, *J* = 5 Hz **CH$_2$**O), 3.98 (s, 1.5H, **CH$_3$**O), 3.90 (s, 1.5H, **CH$_3$**O), 3.62–3.57 (m, 3H, 1 × **CH$_2$**N and 0.5 × **CH$_2$**N), 3.51–3.49 (t, *J* = 5 Hz, 1H, **CH$_2$**N), 3.13–3.10 (m, 2H, **CH$_2$**N), 2.99 (s, 3H, **CH$_3$**N), 2.92 (s, 3H, **CH$_3$**N), 2.48–2.45 (m, 2H, **CH$_2$**(CH_3)), 0.92–0.89 (m, 3H, **CH$_3$**(CH_2)) ppm. ^{13}C NMR (500 MHz, CD_3OD): δ 219.01, 182.33, 133.18, 131.77, 130.86, 128.94, 127.18, 115.70, 115.44, 114.88, 114.59, 112.44, 69.92, 63.08, 56.99, 43.83, 40.93, 37.96, 27.55, 13.84 ppm. UV–vis (0.13 mM, 10% aq MeOH): λ_{max} = 238 nm (ε = 1685 $M^{-1}cm^{-1}$), 295 nm (ε = 768 $M^{-1}cm^{-1}$), 340 nm (ε = 390 $M^{-1}cm^{-1}$).

II. Synthesis of ONB$_2$-4OHT 2 (Scheme 2)

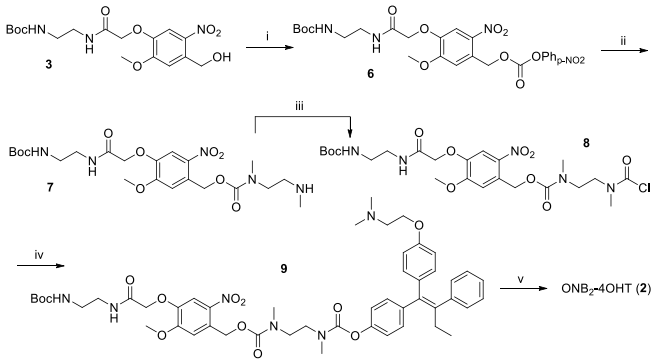

Reagents and Conditions: i) *p*-nitrophenyl chloroformate, DIPEA, $CHCl_3$, 0°C to rt; ii) *N,N'*-dimethylethylenediamine, Et_3N, CH_2Cl_2; iii) triphosgene, Et_3N, CH_2Cl_2; iv) (Z/E)-4OHT, 4-dimethylaminopyridine (DMAP), DMF, 5°C to rt; v) CF_3CO_2H/CH_2Cl_2 (1:1), rt, 30 min

6: To a cold solution of *p*-nitrochloroformate (0.529 g, 2.63 mmol) dissolved in anhydrous THF (15 mL) was added a solution of 3 (1.0 g, 2.51 mmol) and *N*,*N*-diisopropylethylamine (DIPEA; 0.916 mL) dissolved in $CHCl_3$ (15 mL). This mixture was stirred at 5 °C for 30 min and at room temp overnight. A second portion of *p*-nitrophenylchloroformate (0.529 g) was added to the reaction mixture followed by the addition of dimethylaminopyridine (DMAP, 0.321 g, 2.63 mmol). The final mixture was stirred at room temp for additional 4 h, and concentrated *in vacuo*. The residue was dissolved in ethyl acetate (300 mL), and washed with 1M H_3PO_4, a saturated $NaHCO_3$ solution and finally a brine solution. The organic phase was collected, dried over Na_2SO_4, and evaporated to dryness, yielding S4 as pale yellow solid (1.9 g). R_f (2:1 EtOAc/hexane) = 0.44. ^{1}H NMR (500 MHz, $CDCl_3$): δ 8.31–8.30(dd, J_1 = 2 Hz, J_2 = 7 Hz, 2H, ArH (ortho to NO_2; Ph_{NO2})), 7.81 (s, 1H, ArH (ortho to NO_2; ONB)), 7.43–7.41 (dd, J_1 = 2 Hz, J_2 = 7 Hz, 2H, ArH (meta to NO_2; Ph_{NO2})), 7.17 (s, 1H, ArH meta to NO_2), 5.72 (s, 2H, $ArCH_2OC(=O)$), 4.90 (br, 1H, NH), 4.60 (s, 2H, $ArOCH_2C(=O)$), 4.04 (s, 3H, OCH_3), 3.51–3.48 (m, 2H, $CH_2NHC(=O)$), 3.34–3.32 (m, 2H, CH_2NHBoc), 1.42 (s, 9H, NHBoc) ppm.

7: To a solution of **6** (0.258 mg, 0.457 mmol) dissolved in tetrahydrofuran (10mL) cooled in an ice-water bath was added *N,N'*-dimethylethylenediamine (100.8mg, 1.143mmol). The mixture was stirred in the ice-water bath for 2 h, and concentrated *in vacuo*. This crude product was purified by flash silica column chromatography by eluting with 10% MeOH/CH_2Cl_2, affording **7** as pale yellow solid (78.6 mg, 33% yield). R_f (10% MeOH/CH_2Cl_2) = 0.12. MS (ESI) *m/z* (relative intensity, %) = 514.1 (100) $[M+H]^+$, 458.0 (33). ^{1}H NMR (500 MHz, CD_3OD): δ 7.73 (s, 1H, ArH ortho to NO_2), 7.19 (br, 1H, ArH meta to NO_2), 7.10 (s, 1H), 5.52 (s, 2H, Ar**CH$_2$**OC(=O)), 4.90 (br, 1H), 4.57 (s, 2H, ArO**CH$_2$**C(=O)), 3.99 (s, 3H, **OCH$_3$**), 3.50–3.47 (m, 4H), 3.33–3.31 (m, 2H), 3.03–2.98 (m, 3H), 2.85–2.78 (m, 2H), 2.498–2.445 (m, 3H), 1.419 (s, 9H, *N*H**Boc**) ppm. ^{13}C NMR (100 MHz, $CDCl_3$): δ 196.28, 187.96, 167.91, 156.44, 153.96, 145.63, 139.56, 115.18, 111.77, 111.25, 110.73, 79.57, 68.88, 64.00, 56.24, 49.65, 49.21, 48.52, 40.22, 39.72, 36.34, 36.05, 35.14, 34.53, 28.25 ppm.

8: To a cold solution of **7** (9.8 mg, 0.0191 mmol) dissolved in dichloromethane (1 mL) cooled in an ice bath was added

triethylamine (16 μL, 0.11 mmol) and triphosgene (5.7 mg, 0.019 mmol). The mixture was stirred at 5°C for 40 min, concentrated *in vacuo*, and purified by flash silica column chromatography eluting with 2–5% MeOH/CH_2Cl_2. The desired product **8** was isolated as pale yellow solid (13.7 mg). R_f (5% MeOH/CH_2Cl_2) = 0.42.

9 (*N*-Boc protected ONB_2-4OHT): 4OHT (9.4 mg, 24.3 μmol) was dissolved in a mixture of DMF and dichloromethane (2 mL, 1:1) containing triethylamine (19.6 μL, 142 μmol) and 4-dimethylaminopyridine (3.0 mg, 24.6 μmol). This solution was cooled in an ice bath (5°C), and followed by the addition of **8** (13.5 mg, 23.5 μmol) dissolved in a mixture of DMF and dichlromethane (0.3 mL, 1:1). The final mixture was stirred in the ice bath for 30 min, and at room temp overnight. It was concentrated *in vacuo*, and the residue was purified by flash silica column chromatography by eluting with 2–10% MeOH/CH_2Cl_2. The desired product **9** was isolated as pale yellow solid (9.5 mg, 44% yield). R_f (5% MeOH/CH_2Cl_2) = 0.50. HPLC: t_R = 11.68, 11.84 min; purity >98%. MS (ESI) *m/z* (relative intensity, %) = 927.8 (100) $[M+H]^+$. HRMS (ESI) calcd for C49H63N6O12 $[M+H]^+$ 927.4498, found 927.4507. ^{1}H NMR (500 MHz, CD_3OD): δ 7.83–7.74 (m, 1H, ArH ortho to NO_2), 7.23–7.17 (m, 1H, ArH ortho to NO_2), 7.15–6.94 (m, 9H, ArH), 6.81–6.55 (m, 4H, ArH), 5.52–5.47 (m, 1H, Ar**C**$\mathbf{H_2}$O), 5.43–5.35 (m, 1H, Ar**C**$\mathbf{H_2}$O), 4.60-4.55 (m, 2H, ArO**C**$\mathbf{H_2}$C(=O)), 4.15-4.12 (t, *J* = 5.5 Hz, 1H, **C**$\mathbf{H_2}$O), 3.98–3.96 (t, *J* = 5.5 Hz, 1H, **C**$\mathbf{H_2}$O), 3.91–3.78 (m, 3H, **C**$\mathbf{H_3}$**O**), 3.68–3.50 (m, 4H, 2 × **C**$\mathbf{H_2}$N), 3.35–3.33 (m, 2H, **C**$\mathbf{H_2}$N(CH_3)), 3.19–3.17 (m, 2H, **C**$\mathbf{H_2}$N(CH_3)), 3.13–2.84 (m, 6H, 2 × **C**$\mathbf{H_3}$(CH_2)), 2.82–2.80 (m, 1H, **C**$\mathbf{H_2}$N), 2.72–2.70 (m, *J* = 5.5 Hz, 1H, **C**$\mathbf{H_2}$N), 2.47–2.44 (m, 2H, **C**$\mathbf{H_2}$(CH_3)), 2.37 (s, 3H, **C**$\mathbf{H_3}$N), 2.31 (s, 3H, **C**$\mathbf{H_3}$N), 1.44 (s, 4.5H, NH**Boc**), 1.398 (s, 4.5H, NH**Boc**), 0.92–0.87 (m, 3H, **C**$\mathbf{H_3}$(CH_2)) ppm. ^{13}C NMR (100 MHz, $CDCl_3$): δ 187.99, 184.63, 162.94, 132.12, 131.85, 130.80, 130.53, 129.64, 127.85, 115.14, 114.61, 114.06, 113.80, 113.32, 67.35, 45.65, 28.28, 19.54 ppm.

2 (ONB_2-4OHT): To *N*-Boc protected ONB_2-4OHT **9** (5 mg) was added slowly a mixture of trifluoroacetic acid (TFA) and dichloromethane (1:1; 3 mL). The solution was stirred at room temp for 30 min, and evaporated to dryness. The residue was dissolved in 20% aq acetonitrile solution (2 mL), and freeze-dried, yielding pale beige fluffy solid. HPLC: t_R = 10.03, 10.16 min; purity >98% (quantitative deprotection). MS (ESI) *m/z* (relative intensity, %) = 827.4 (76) $[M+H]^+$, 502.3 (100). ^{1}H NMR (500 MHz, CD_3OD): δ 7.83–7.77 (m, 1H, ArH ortho to NO_2), 7.24–7.21 (m, 1H, ArH ortho to NO_2), 7.20–7.01 (m, 9H, ArH), 6.84–6.65 (m, 4H, ArH), 5.51–5.45 (m, 1H, Ar**C**$\mathbf{H_2}$O), 5.44–5.36 (m, 1H, Ar**C**$\mathbf{H_2}$O), 4.66–4.63 (m, 2H, ArO**C**$\mathbf{H_2}$C(=O)), 4.38–4.36 (t, *J* = 5.5 Hz, 1H, **C**$\mathbf{H_2}$O), 4.21–4.19 (t, *J* = 5 Hz, 1H, **C**$\mathbf{H_2}$O), 3.95–3.86 (m, 3H, **C**$\mathbf{H_3}$**O**), 3.62–3.50 (m, 6H, 2 × **C**$\mathbf{H_2}$N and **C**$\mathbf{H_2}$N(CH_3)), 3.14-2.84 (m, 16H, **C**$\mathbf{H_2}$N(CH_3), 2 × **C**$\mathbf{H_3}$(CH_2), **C**$\mathbf{H_2}$N and 2 × **C**$\mathbf{H_3}$N), 2.47–2.44 (m, 2H, **C**$\mathbf{H_2}$(CH_3)), 0.92–0.88 (m, 3H, **C**$\mathbf{H_3}$(CH_2)) ppm. UV–vis (0.11 mM, 10% aq MeOH): λ_{max} = 238 nm (ε = 469 $M^{-1}cm^{-1}$), 295 nm (ε = 311 $M^{-1}cm^{-1}$), 340 nm (ε = 171 $M^{-1}cm^{-1}$).

III. Photochemical 4OHT release in solution (Figure 1b,c). 4OHT release studies were carried out using UV lamps (model XX-15A, Spectroline®) emitting UVA light (wavelength = 320–400 nm) with a peak intensity at 365 nm. ONB_1-4OHT (**1**) or ONB_2-4OHT (**2**) was dissolved in 10% aq MeOH at 0.1 mg/mL. Each solution (3 mL) was loaded in a glass Petri dish (diameter = 5 cm) and exposed to UV light at the distance of ~5 cm from lamps. Kinetics of drug release was investigated by taking aliquots (0.4 mL each) at various time points as specified in each Figure. The aliquots were analyzed by analytical HPLC, UV–vis spectrophotometry, and ESI mass spectrometry.

IV. UT MEFs. Mouse embryonic fibroblasts (MEFs) containing a UBC-$CreER^{T2}$ transgene and the mTmG reporter (UT MEFs) were previously generated.[22] UT MEFs were maintained in media containing Dulbecco's modified Eagle's medium (DMEM) high glucose (GIBCO) and supplemented with 10% FBS (Invitrogen), 100 U/mL Penicillin 100 μg/mL Streptomycin (Hyclone), and 1x L-glutamine (Hyclone). Cells were passaged 1:3 with 0.05% Trypsin (Gibco) every 3-5 days and were used below 8 passages. For spatial activation (Figure 4), UT MEFs were plated onto 50 mm glass bottom tissue culture dishes (EMS, #70674-52).

V. ACRL MEFs. 4OHT-inducible ACRL reporter MEFs were generated by crossing two transgenic mouse lines: 1) Actin-$CreER^{Rainbow}$ mice with both a constitutively active chicken β-actin promoter driving expression of CreER[29] as well as the Rainbow reporter construct,[31] and 2) another mouse line with a LacZ reporter inserted into constitutively active Rosa26 locus.[30] Actin-Cre-$ER^{Rainbow}$ X LacZ e14.5 embryos were harvested, then heads and livers were removed and remaining tissue was minced and treated with 0.05% Trypsin (Gibco) and plated onto gelatinized tissue culture dishes. ACRL MEFs were maintained as described above.

VI. LacZ Expression. Following treatment with 4OHT or ONB_1-4OHT, ACRL MEFs were fixed using 0.2% glutaraldehyde (Sigma) for 30 min then washed 3x with PBS for 5 min. LacZ buffer containing 1 mM magnesium chloride (Sigma), 3 mM potassium ferricyanide (Sigma), 3 mM potassium hexacyanoferrate (Sigma), 0.02% tween, and X-gal (VWR) was added to ACRL MEFs overnight at 37°C. Cells were washed the next day 3x with PBS for 5 min and imaged using a Nikon Eclipse Ti Inverted Fluorescent Imaging microscope with NIS-Elements software.

VII. Photochemical release in UT MEF cells and confocal microscopy (Figure 1d). UT MEFs below passage 5 were seeded on two 8-chamber coverglass slides (Thermo-scientific) at 1 × 10^5 cells/well in complete media overnight. 5 mM dilutions of 4OHT, ONB_1-4OHT **1**, and ONB_2-4OHT **2** were prepared in culture media. Growth medium was removed from the cells, and 250 μL of each 4OHT solution was added to the respective wells. Cells were incubated at 37 °C for 5 min, and one slide was exposed to a UVA lamp (Spectroline XX-15A long wave UV lamp, mean wavelength = 365 nm) for 5 min, while the other was kept in the dark at room temp. 250 mL of fresh media was added to each well, and cells were incubated for 24h at 37°C. Cells were washed 2× with PBS and fixed in 4% paraformaldehyde in PBS for 10 min, dried and mounted in ProLong gold with DAPI. Images were taken on a Leica inverted SP5X confocal fluorescence microscope (Leica Microsystems, Buffalo Groves, IL) with 40× magnification in sequential scanning

mode (mTomato ex 555 nm, em 570-650 nm, GFP ex 488 nm, em 500-540 nm, and DAPI ex 350 nm, em 450-490 nm).

VIII. Treatment of UT MEFs and ACRL MEFs with 4OHT and ONB-4OHT. Hydroxytamoxifen (4OHT) (Sigma, H7904) was resuspended in DMSO to 8 mM, then further diluted in MEF media and added to UT MEFs. ONB_1-4OHT **1** and ONB_2-4OHT **2** were resuspended in water to 8 mM, and stored at −80 °C. UV light was provided by a 6-watt 2UV Transilluminator (UVP Model LM-20E) with a wavelength of 365nm (longwave, UV-A). The UV light source was placed upside-down; approximately 3 cm above either MEF media containing ONB_1-4OHT or UT and ACRL MEFs pretreated with ONB_1-4OHT. For 24 h treatments of UT and ACRL MEFs with ONB_1-4OHT (Figure 1), ONB_1-4OHT was diluted in media, uncaged with UV light, and added to UT and ACRL MEFs. For pretreatment experiments (Figures 2 and 3), ONB_1-4OHT was diluted in media and added to UT and ACRL MEFs for 1 h. Cells were washed with PBS, exposed dry to UV light for indicated times, then incubated in fresh media for 24 h. UT and ACRL MEFs were imaged with a Nikon Eclipse Ti Inverted Fluorescent Imaging microscope with NIS-Elements software. UT and ACRL MEFs were harvested with Trypsin (GIBCO) and UT MEFs were analyzed for Tomato/GFP expression and ACRL MEFs were analyzed for Tomato, GFP, CFP, and OFP expression by flow cytometry on a BD FACSAria-II (BD Biosciences) and Flowjo software (Treestar).

Acknowledgements

The authors wish to thank Vanessa Scarfone, Amanda Dickson and the UCI Stem Cell Research Center Core for FACS and microscopy assistance, and Connie Inlay for lab management. Part of this work was supported by the Michigan Nanotechnology Institute for Medicine and Biological Sciences, the University of Michigan Office of the Vice President for Research, and Shanghai Jiao Tong University (SKC). The UCI Stem Cell Core is supported in part by a grant from the California Institute for Regenerative Medicine (CL1-00520-1.2).

Notes and references

[1]*Sue and Bill Gross Stem Cell Research Center, University of California Irvine, Irvine, CA 92697, USA*
[2]*Department of Molecular Biology and Biochemistry, University of California Irvine, Irvine, CA 92697, USA*
[3]*Department of Internal Medicine, Michigan Nanotechnology Institute for Medicine and Biological Sciences, University of Michigan, Ann Arbor, MI 48109, USA*
[4]*Department of Medicine, Division of Endocrinology, University of California Irvine, Irvine, CA 92697, USA*

[†]*equal contributing authors: Tannaz Faal and Pamela T. Wong*

**corresponding authors: Seok Ki Choi (skchoi@med.umich.edu) and Matthew A. Inlay (minlay@uci.edu)*

Electronic Supplementary Information (ESI) available: This includes detailed methods, chemistry and syntheses, photochemical release kinetics, and supplementary figures. See DOI: 10.1039/c000000x/

1 R. Feil, *Handb Exp Pharmacol*, 2007, 3-28.
2 D. Metzger, J. Clifford, H. Chiba and P. Chambon, *Proc Natl Acad Sci U S A*, 1995, **92**, 6991-6995.
3 R. Feil, J. Brocard, B. Mascrez, M. LeMeur, D. Metzger and P. Chambon, *Proc Natl Acad Sci U S A*, 1996, **93**, 10887-10890.
4 R. Feil, J. Wagner, D. Metzger and P. Chambon, *Biochem Biophys Res Commun*, 1997, **237**, 752-757.
5 E. Nakamura, M. T. Nguyen and S. Mackem, *Dev Dyn*, 2006, **235**, 2603-2612.
6 A. Banerjee, K. Lee and D. E. Falvey, *Tetrahedron*, 1999, **55**, 12699-12710.
7 G. Mayer and A. Heckel, *Angew Chem Int Ed Engl*, 2006, **45**, 4900-4921.
8 A. V. Pinheiro, P. Baptista and J. C. Lima, *Nucleic Acids Res*, 2008, **36**, e90.
9 S. K. Pollitt and P. G. Schultz, *Angew Chem Int Edit*, 1998, **37**, 2104-2107.
10 A. V. Karginov, Y. Zou, D. Shirvanyants, P. Kota, N. V. Dokholyan, D. D. Young, K. M. Hahn and A. Deiters, *J Am Chem Soc*, 2011, **133**, 420-423.
11 D. S. Miller, S. Chirayil, H. L. Ball and K. J. Luebke, *Chembiochem*, 2009, **10**, 577-584.
12 E. A. Lemke, D. Summerer, B. H. Geierstanger, S. M. Brittain and P. G. Schultz, *Nat Chem Biol*, 2007, **3**, 769-772.
13 N. K. Mal, M. Fujiwara and Y. Tanaka, *Nature*, 2003, **421**, 350-353.
14 S. S. Agasti, A. Chompoosor, C. C. You, P. Ghosh, C. K. Kim and V. M. Rotello, *J Am Chem Soc*, 2009, **131**, 5728-5729.
15 S. K. Choi, T. Thomas, M. H. Li, A. Kotlyar, A. Desai and J. R. Baker, Jr., *Chem Commun (Camb)*, 2010, **46**, 2632-2634.
16 Y. Shamay, L. Adar, G. Ashkenasy and A. David, *Biomaterials*, 2011, **32**, 1377-1386.
17 K. H. Link, Y. Shi and J. T. Koh, *J Am Chem Soc*, 2005, **127**, 13088-13089.
18 Y. Shi and J. T. Koh, *Chembiochem*, 2004, **5**, 788-796.
19 D. K. Sinha, P. Neveu, N. Gagey, I. Aujard, T. Le Saux, C. Rampon, C. Gauron, K. Kawakami, C. Leucht, L. Bally-Cuif, M. Volovitch, D. Bensimon, L. Jullien and S. Vriz, *Zebrafish*, 2010, **7**, 199-204.
20 D. K. Sinha, P. Neveu, N. Gagey, I. Aujard, C. Benbrahim-Bouzidi, T. Le Saux, C. Rampon, C. Gauron, B. Goetz, S. Dubruille, M. Baaden, M. Volovitch, D. Bensimon, S. Vriz and L. Jullien, *Chembiochem*, 2010, **11**, 653-663.
21 W. F. Edwards, D. D. Young and A. Deiters, *ACS Chem Biol*, 2009, **4**, 441-445.
22 M. A. Inlay, V. Choe, S. Bharathi, N. B. Fernhoff, J. R. Baker, Jr., I. L. Weissman and S. K. Choi, *Chem Commun (Camb)*, 2013, **49**, 4971-4973.
23 S. K. Choi, T. P. Thomas, M. H. Li, A. Desai, A. Kotlyar and J. R. Baker, Jr., *Photochem Photobiol Sci*, 2012, **11**, 653-660.
24 S. K. Choi, M. Verma, J. Silpe, R. E. Moody, K. Tang, J. J. Hanson and J. R. Baker, Jr., *Bioorg Med Chem*, 2012, **20**, 1281-1290.
25 Y. Ruzankina, C. Pinzon-Guzman, A. Asare, T. Ong, L. Pontano, G. Cotsarelis, V. P. Zediak, M. Velez, A. Bhandoola and E. J. Brown, *Cell Stem Cell*, 2007, **1**, 113-126.
26 M. D. Muzumdar, B. Tasic, K. Miyamichi, L. Li and L. Luo, *Genesis*, 2007, **45**, 593-605.
27 W. M. Meylan, P. H. Howard and R. S. Boethling, *Environ. Toxicol. Chem.*, 1996, **15**, 100-106.
28 B. Huang, S. Tang, A. Desai, X. M. Cheng, A. Kotlyar, A. Van Der Spek, T. P. Thomas and J. R. Baker, Jr., *Bioorg Med Chem Lett*, 2009, **19**, 5016-5020.
29 C. Guo, W. Yang and C. G. Lobe, *Genesis*, 2002, **32**, 8-18.
30 P. Soriano, *Nat Genet*, 1999, **21**, 70-71.
31 K. Red-Horse, H. Ueno, I. L. Weissman and M. A. Krasnow, *Nature*, 2010, **464**, 549-553.
32 X. Wang, X. Chen and Y. Yang, *Nat Methods*, 2012, **9**, 266-269.
33 D. D. Yu and B. M. Forman, *J Org Chem*, 2003, **68**, 9489-9491.

